Chapter

Performance Analysis of a New Combined Organic Rankine Cycle and Vapor Compression Cogeneration and Tri-Generation and Water Desalination

Noureddine Toujani, Nahla Bouaziz and Lakder Kairouani

Abstract

The new ORC-VCC combined system is analyzed. It is a new system that can be operated in four modes depending on the type of energy. The novelty of the system appears essentially in the development of new ORC-VCC combination architecture, the lowering of the condensation temperature, the possibility of cold production by the ORC cycle affected by the pumping phase, preheating of fluid cycle using the VCC cycle fluid, and new configurations based on the integration of heat recovery systems to improve overall system performance. In addition, each installation mode has several configurations depending on the recovery points that will be integrated later, besides its adaptation to any energy source, where we can use biomass, solar, and heat rejects of industry at low temperatures (60–130°C). This system can produce under and above zero temperature. Although, due to its architecture, it is also characterized by many combination of selection fluid for the ORC and VCC cycles, it is not necessary to have the same working fluid as in the classic systems. In this study, three configurations are examined and studied in terms of energy efficiency mainly the performance of each configuration including net power, refrigeration capacity and overall efficiency, the thermal efficiency for ORC.

Keywords: organic Rankine cycle, tri-generation, vapor compression cycle, desalination of seawater

1. Introduction

According to the International Energy Agency (IEA), solar power will be the fastest-growing source of energy in the future. The growth rate of solar energy can reach more than 12% [1]. Many countries today are making decisions to put political strategies in the use of renewable resources. For that, many studies were done all over the world, Asia [2, 3], Africa [4, 5], and America [6], whose objectives are to determine the energy potential and to choose the political strategies to improve the solar energy potential. In Europe [1], the Commission communication to the European Parliament and the Council for new European energy policies set out in

2014 [7] a target to reach 20% energy efficiency by 2020 and 30% by 2030. In fact, researches are looking for technologies that can be used to mitigate global warming around the world and reduce CO_2 emissions [8]. Energy shortage problems are faced in all over the world and becoming more acute in all fields [9, 10] (metallurgy, chemical, electrical and mechanical sectors). So, the world is facing two energy challenges: increase production to meet energy needs and reduce CO_2 emissions issued by industrial plants. For that, the utilization of renewable energy becomes a political duty and not a strategic choice to solve energy problems. Among these renewable resources used is the solar energy: Sunil Kumar [11] published a review as a synthetic fruit of studies done on energy analysis. He presented the various solar energy systems used in solar drying [12, 13], solar air conditioning [14, 15], solar refrigeration [16], solar water heating [17], and solar cooking [18]. These systems have been operated by solar photovoltaic techniques [19] and solar thermal energy used for heat and power generation [20–22].

In terms of management and tri-generation system design, several studies [23–28] analyzed the energy potential through the integration and hybridization of renewable sources.

The new ORC-VCC combined system is developed. As it is shown in **Figures 1–4**, we wanted to design a new architecture for multi-objective optimization. It is a new system that can be operated in four modes depending on the type of the produced energy, namely, the electric energy, refrigeration, poly-generation, and water desalination. The four developed modes are:

- **Mode 1**: cold production. **Figure 1** illustrates the basic architecture of the system. It receives a heat flow from an external renewable source in the boiler so that the ORC cycle can be run in order to deliver a mechanical work at the turbine; this work is transmitted totally to the VCC cycle compressor (turbo system compressor). This system provides us a refrigeration quantity at the evaporator as illustrated in the figure.

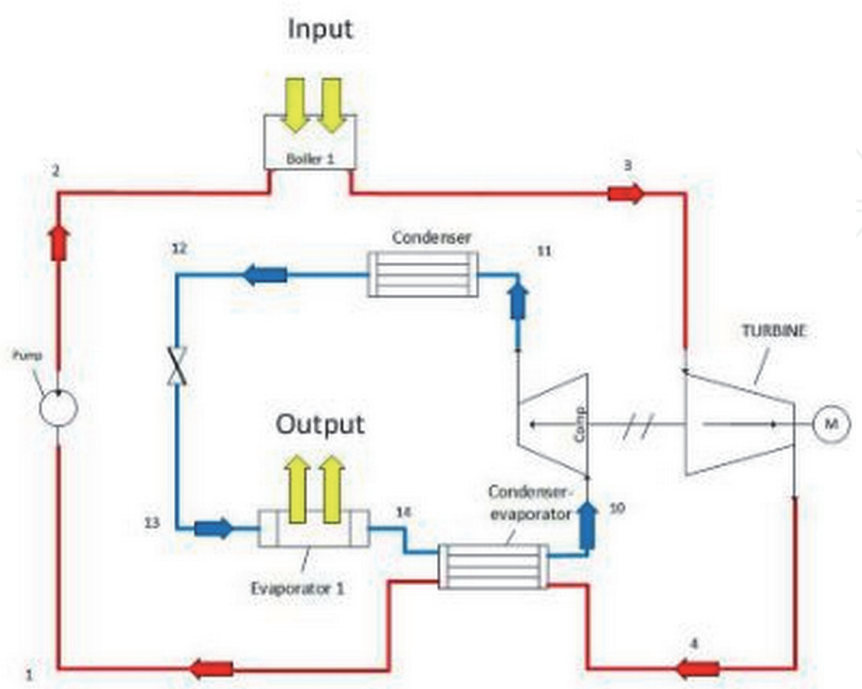

Figure 1.
Cold production mode.

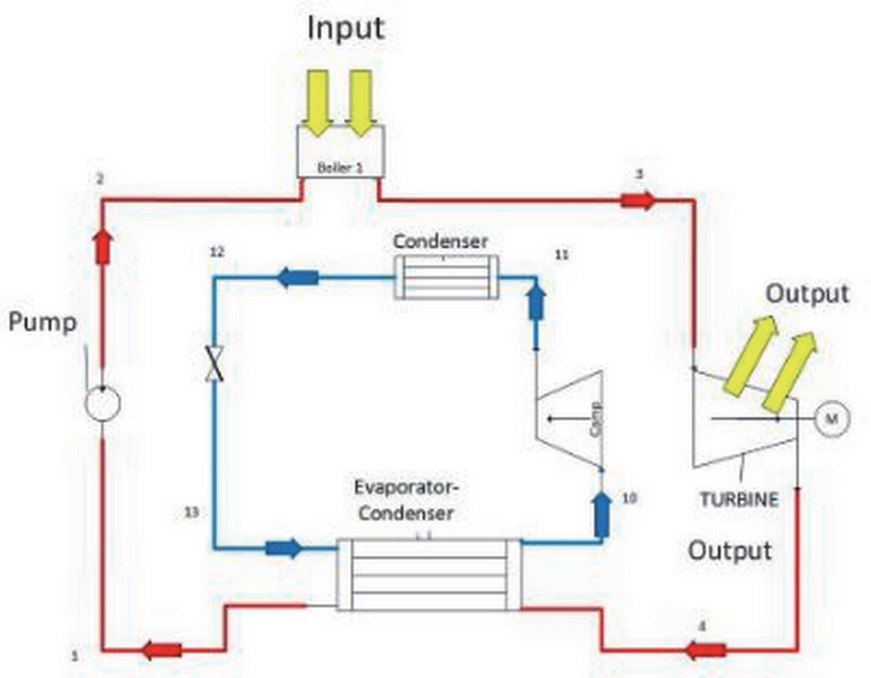

Figure 2.
Electricity production mode.

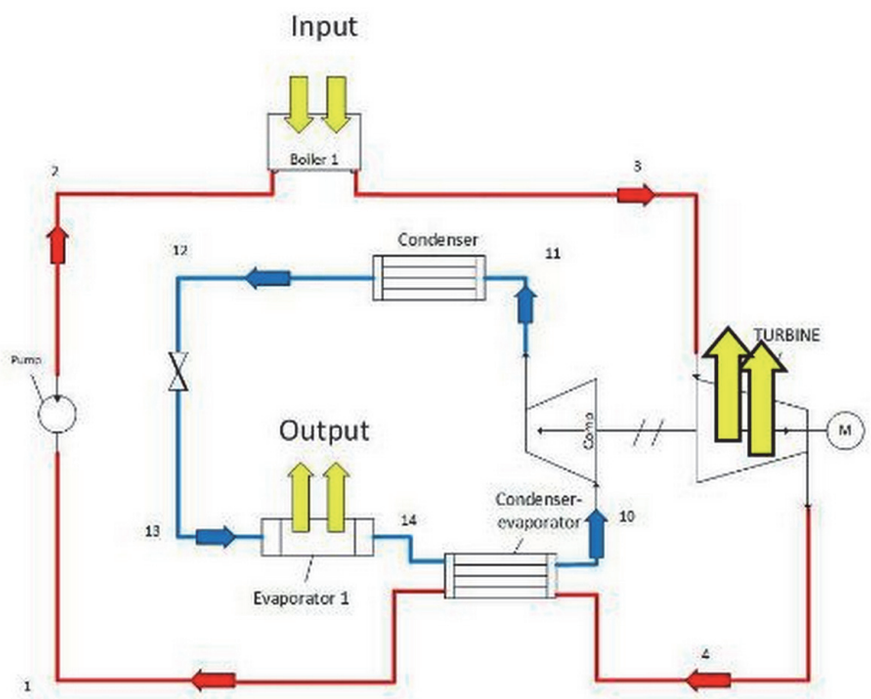

Figure 3.
Cogeneration production mode.

- **Mode 2**: electricity power. **Figure 2** shows the basic installation. It also receives a quantity of heat from an external renewable source in the boiler to have mechanical work at the turbine; it is partially transmitted to the VCC cycle compressor. On the other hand, the power supplied by the VCC cycle evaporator is totally exploited by the ORC cycle condenser. So this mode of operation requires a renewable source and provides us an electric power.

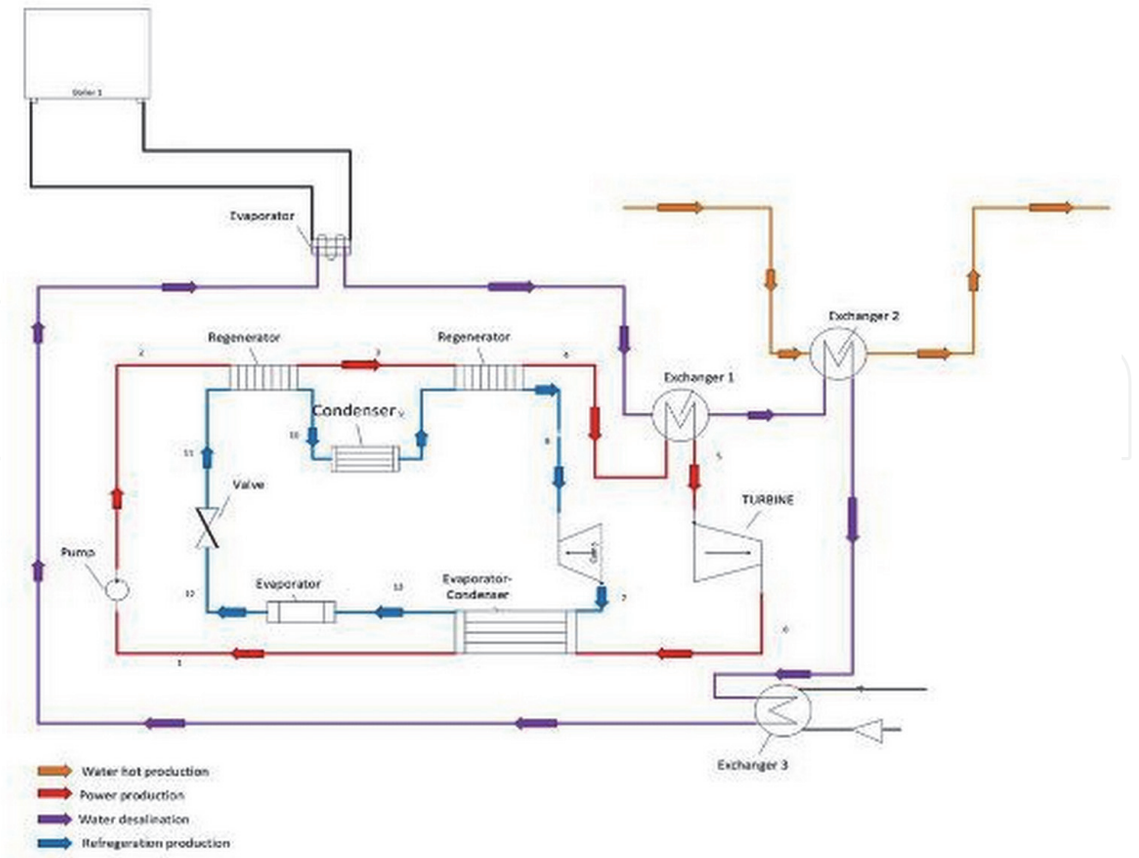

Figure 4.
Tri-generation and desalination mode.

- **Mode 3**: cogeneration (cold production and electricity power). **Figure 3** presents the basic architecture. It receives an external renewable source in the boiler. Through this source, it allows us to have mechanical work at the turbine: this is partially transmitted to the VCC cycle compressor as mode 2. The power provided by the VCC cycle evaporator is partially operated by the condenser ORC cycle. So this operation mode requires a renewable source and offers an electric power by ORC cycle and cooling capacity by the VCC cycle.

- **Mode 4**: tri-generation and desalination of seawater are illustrated in **Figure 4**. This configuration has four circuits: an ORC cycle circuit that is represented by the red color, a circuit of the VCC cycle in blue, a circuit in purple color of the desalinated seawater, and a red circuit of the heated water. We will couple the system with a limited renewable energy source.

In addition, each installation mode has several configurations depending on the recovery points that will be integrated later, besides its adaptation to any energy source, where we can use biomass, solar, and heat rejects of industry at low temperatures (60–130°C). This system could produce a negative and a positive cold. Although, due to its architecture, it is also characterized by many combinations of selection fluid for the ORC and VCC cycles, it is not necessary to have the same working fluid as the classic systems.

The main purpose of this presented study is to analyze the performance of a new system that combines the steam compression cycle and the Rankine cycle for tri-generation (electricity, cold, hot) as well as the desalination of water. This system uses a low-temperature heat source such as solar energy, heat from industrial waste, and biomass.

The objectives of this study are:

- Architectural development of the basic system
- Development of improvement configurations
- Energy analysis and choice of fluids
- The impact of operating parameters on energy performance

In this study, we will develop a new ORC combination with the VCC system in order to make cogeneration and tri-generation with a negative temperature cold (−10°C, 0°C), as well with a positive temperature cold (0°, 10°C). Three new configurations are examined and studied in terms of energy efficiency, namely, the performance of each configuration including net power, refrigeration capacity and overall efficiency, the thermal efficiency for ORC, and the coefficient of performance for VCC. The working fluids are n-hexane for ORC and R600 for VCC.

2. System description

As illustrated in **Figure 5**, the configuration consists of four circuits: an ORC cycle circuit represented by the red color, a circuit of the VCC cycle which is in blue, a circuit in purple color of the desalinated seawater, and a red circuit in the heated water. We will couple our facility with a limited renewable energy source which is thermal photovoltaic center, at low temperature (100–130°C). Our approach is to lower the condensing temperature between −10 and 10°C of the ORC cycle so that the delivered work can be increased. So, a cold part produced by VCC will be dedicated to condense the fluid of the ORC cycle. For this, we will integrate an exchanger regenerator1 which is used to condense the ORC fluid by a quantity of cold produced laying vapor phase VCC side.

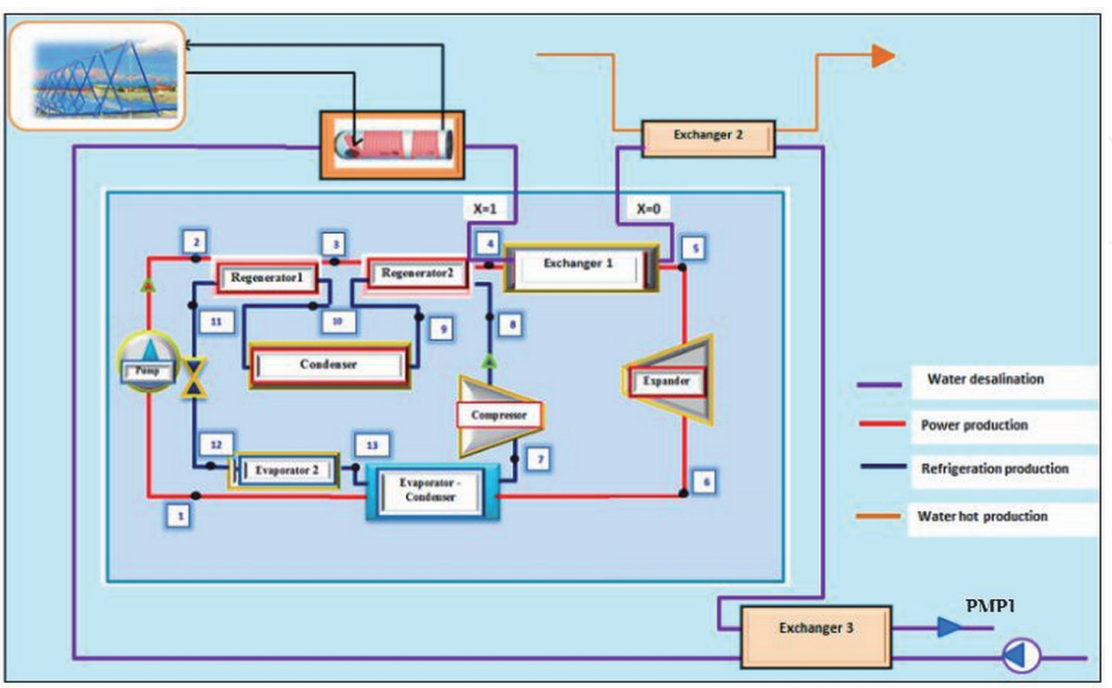

Figure 5.
System of study.

2.1 Desalinated water circuit description

First, the seawater is pumped by a pump PMP1 and preheated by the **exchanger 3**. Then, it will be evaporated at constant pressure in the boiler by a solar collector. After having saturated steam, the latter passed the condensation phase using the **regenerator 2** in order to equate the water at a hot temperature which is equal to that of the evaporation. With integrity of exchanger H2, we started the first phase of cooling the salty water and chaffered sanitary water. In the end, for the desalted water to complete this phase of cooling, also we have to warm the water out of the sea, using an exchanger H3.

2.2 Circuit description of heated domestic water

This is the simplest circuit in our loop. It is enough the sanitary water enters the exchanger H3 to become hot thanks to the quantity of heat provided by the desalted water.

So our system produces electricity due to the mechanical work obtained by the turbine, a refrigeration quantity by the evaporator 1, and de-watered water obtained using two serial transformations (evaporation, condensation) and produces hot water by the exploitation of the hot quantity from the de-watered water.

3. The different configurations developed for ORC-VCC combination

3.1 Configuration A

The cycle A is the basic configuration. We will combine the two ORC and VCC cycles without any recovery for cogeneration. As shown in **Figure 6**, the only combination is made at the heat exchanger H1 which serves as the condenser of the ORC cycle fluid. This configuration allows having cogeneration with positive or negative cold according to our needs.

The operating principle is described as follows:

First, the ORC cycle fluid enters the boiler in order to heat it up to 100°C by a renewable external source (biomass, industrial and solar thermal discharge, etc.). It suffices that the fluid reaches a saturated vapor phase; it enters a turbine to generate a mechanical work. This phase allows the fluid to pass from the high pressure to the low pressure. After this phase, a condensation phase is necessary to make the fluid in a liquid state. For our application, the condensation is done at low temperature which requires a cold external source. For this, we combined the ORC cycle condenser with the VCC cycle evaporator by integrating a H1 exchanger. For this configuration, after condensation, the fluid goes to the pumping phase.

In addition, the VCC cycle operation is the inverse of those ORC cycle. The VCC fluid is compressed with a mechanical compressor and then condensed at a temperature of 30°C. In this configuration, after this phase, the fluid is released directly by an expansion valve. Then it is evaporated in two phases.

3.2 Configuration B

For cycle B, we kept the same basic architecture as in cycle A, except that we will integrate an H2 exchanger. This exchanger is mounted just after the pumping phase of the ORC cycle. Seeing that the temperature obtained at the pumping point is

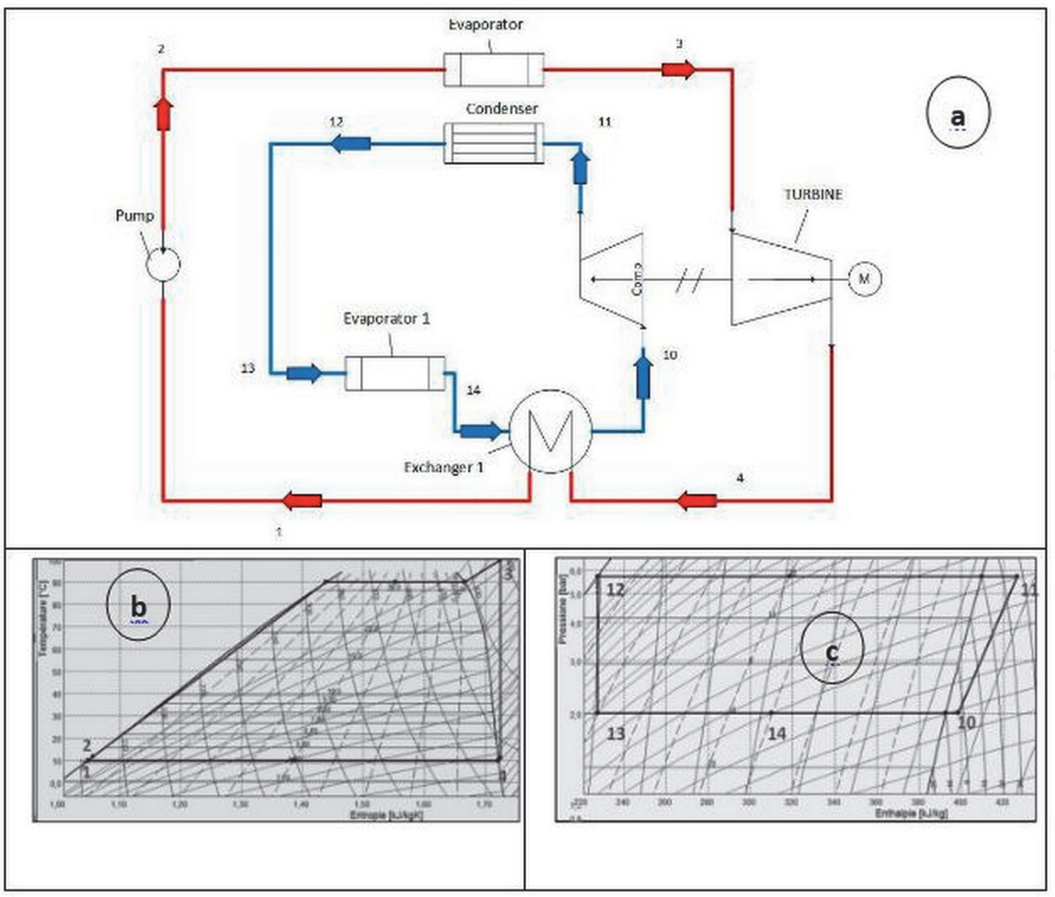

Figure 6.
Schematic and T-S diagrams of the configuration A. (a) Schematic of the configuration A, (b) T-S diagrams for ORC cycle, and (c) P-H diagrams for VCC cycle.

almost the same as the temperature of condensation which varies between −10 and 10°C, the idea is to exploit this temperature to make the sub-cooling of the VCC cycle to improve its performance. Cycle B is shown in **Figure 7**, and it is also developed to make cogeneration with a negative cold.

3.3 Configuration C

As shown in **Figure 8**, cycle C is used also for cogeneration. Unlike the conventional ORC cycle, which is used only for electricity production at the turbine state, cycle C allows the generation of electricity and cold in the ORC cycle. So, the configuration C is used to produce negative cold, positive cold, and electricity.

We will use the heat quantity at low temperature following the pumping step in the ORC cycle in order to produce a positive cold at 18°C for air conditioning. For this reason, we will integrate the H3 exchanger for the heat transfer between the ambient air and the ORC cycle fluid.

4. Mathematical modeling and validation of the model

4.1 Thermodynamic modeling

During this study, we treated the thermodynamic equations as well as the resolution by a calculation program developed by the EES software. Also, this software allows us to realize the different curves and tables presented in the study.

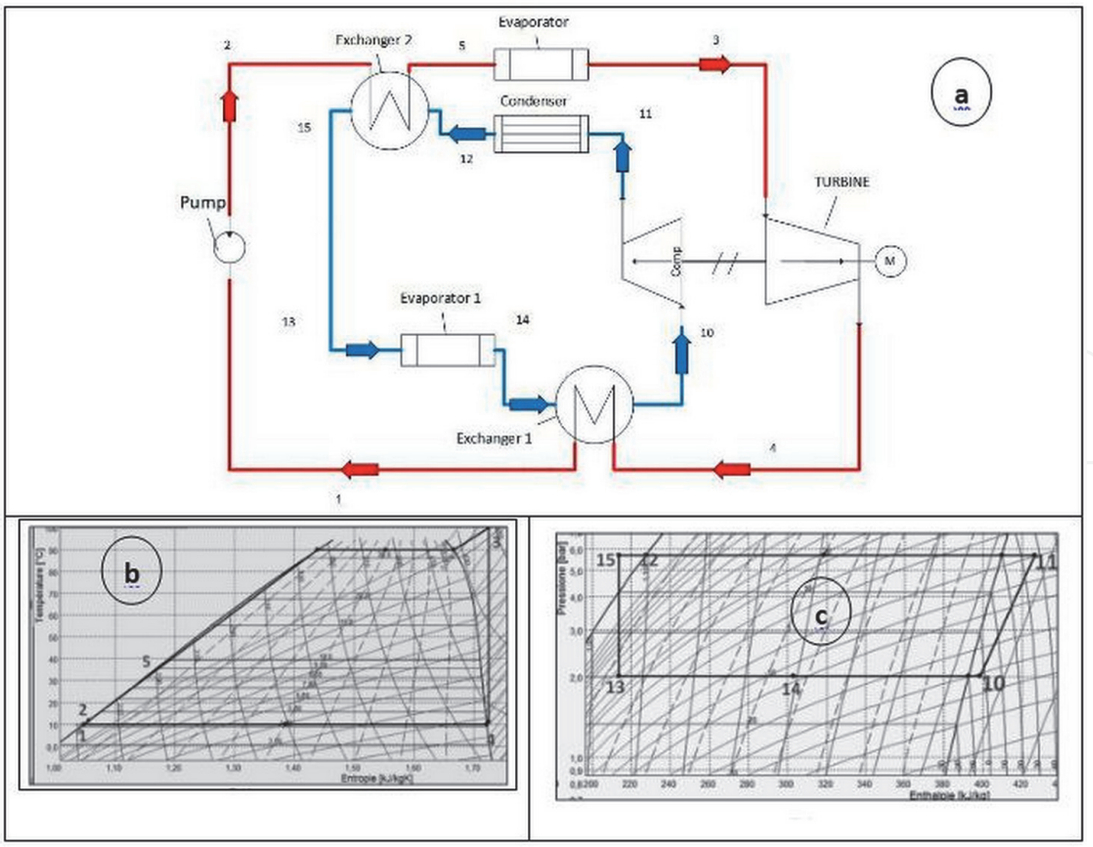

Figure 7.
Schematic and T-S diagrams of the configuration B. (a) Schematic of the configuration B, (b) T-S diagrams for ORC cycle, and (c) P-H diagrams for VCC cycle.

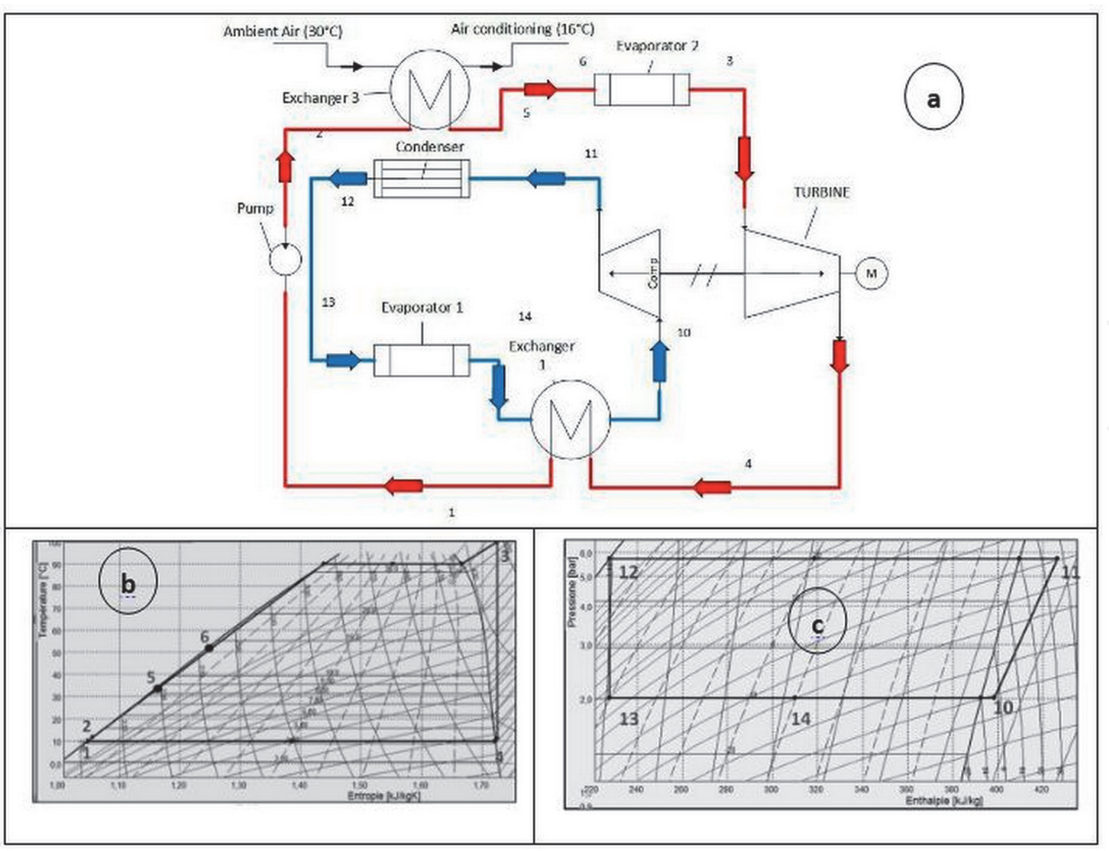

Figure 8.
Schematic and T-S diagrams of the configuration C system. (a) Schematic of the configuration C, (b) T-S diagrams for ORC cycle, and (c) P-H diagrams for VCC cycle.

Table 1 illustrates the different thermodynamic models used throughout the work and the different configurations for cogeneration mode.

4.2 Validation of the model

The approach followed to validate our model is based on two procedures of the developed model. The ORC and the VCC are validated, respectively, in Sections 4.2.1 and 4.2.2.

4.2.1 ORC validation

The model developed for the ORC is tested with the results by Saleh et al. [29], which is the most appropriate configuration to validate the current model using the

ORC	Turbine		$W_T = \dot{m}_1(h_3 - h_{4s}).\eta_{exp}$
	Pump		$W_p = \dot{m}_1 \frac{(h_{2s} - h_1)}{\eta_{pump}}$
	Boiler	(1)	$Q_b = \dot{m}_1(h_3 - h_2)$
		(2)	$Q_b = \dot{m}_1(h_3 - h_5)$
		(3)	$Q_b = \dot{m}_1(h_3 - h_6)$
	Condenser		$Q_{cond} = \dot{m}_1(h_4 - h_1)$
	Thermal efficiency		$\mu_{orc} = \frac{(W_T - W_p)}{Q_b}$
VCC	Compressor		$W_C = \dot{m}_2 \frac{(h_{11s} - h_{10})}{\eta_{comp}}$
	First evaporator		$Q_{ev1} = \dot{m}_2(h_{14} - h_{13})$
	Second evaporator		$Q_{ev2} = \dot{m}_2(h_{10} - h_{14})$
	Overall evaporator		$Q_{ev} = \dot{m}_2(h_{10} - h_{13}) = Q_{ev1} + Q_{ev2}$
	Coefficient of performance		$COP_{VCC} = \frac{(Q_{ev1} + Q_{ev2})}{W_{comp}}$
Overall performance of ORC-VCC	Net work		$W_{net} = W_T - W_p - W_C$
	Overall performance of the system	(1 and 2)	$COP_s = \frac{(Q_{ev1} + W_{net})}{Q_b}$
		(3)	$COP_s = \frac{Q_{ev1} + W_{net} + Q_{hx3}}{Q_b}$
	Efficacity		(1 and 2) $E = \frac{Q_{ev1}}{W_{net}}$
			(3) $E = \frac{Q_{ev1} + Q_{hx3}}{W_{net}}$
	Exchangers for cogeneration	Exchanger 1	$Q_{hx1} = Q_{ev2} = Q_{cond}$
		Exchanger 2	$Q_{hx2} = \dot{m}_1(h_5 - h_2) = \dot{m}_2(h_{12} - h_{15})$
		Exchanger 3	$Q_{hx2} = \dot{m}_1(h_5 - h_2) = \dot{m}_2(h_{16} - h_{17})$
	Exchangers for tri-generation		$Q_{exh3} = \dot{m}_1(h_5 - h_4) = \dot{m}_3(h_{18} - h_{17})$ $Q_{exh4} = \dot{m}_3(h_{19} - h_{18}) = \dot{m}_4(h_{22} - h_{21})$ $Q_{exh5} = \dot{m}_3(h_{20} - h_{19}) = \dot{m}_3(h_{15} - h_{14})$
Mass ratio			$R_1 = m_3/m_4$ $R_2 = m_1/m_4$ $R_3 = m_2/m_4$ $R_4 = m_3/m_4$

Table 1.
Thermodynamic modeling of different configurations ((1) cycle A; (2) cycle B, and (3) cycle C).

Fluid		T4	P_{min}	P_{max}	m_1	η_{orc}
R600	Ref. [30]	48.43	2.85	15.28	17.746	12.58
	Present model	47.83	2.89	15.52	17.58	12.43
	Error	1.23	1.38	1.54	0.93	1.19
R600a	Ref. [30]	45.33	4.038	19.98	2.423	12.12
	Present model	44.61	4.121	19.79	2.371	11.96
	Error	1.58	2.01	0.95	2.14	1.32
R245fa	Ref. [30]	50.7	1.801	12.67	33.424	12.52
	Present model	49.64	1.765	12.81	34.101	12.44
	Error	2.09	1.99	1.09	1.98	0.63

Table 2.
Validation results for ORC cycle.

similar working applied fluid. The comparative results are illustrated in **Table 2**. These results show a small deviation of 2.09% concerning the thermal efficiency. It is worthy to notice that certain changes in the developed model are made for an appropriate comparison. Specifically, the condensation temperature was 40°C and the isentropic efficiency at 85%.

4.2.2 VCC validation

In this section, the operation of the VCC cycle is enabled. Nasir and Kim [31] are selected for the validation. Some changes in the model are made to have an appropriate comparison against the literature. Indeed, the temperature of the condenser is set to 30°C. **Table 3** includes the validation results along with the COP for cooling. We selected three fluids for validation, which are R245fa, R123, and R134a. **Table 3** shows the margin of error between Ref. [31] and our model. The error results for R245fa, R123, and R134a are, respectively, 0.6, 0.44, and 0.92%. These margins are acceptable to give their low values.

Fluid		COPvcc
R245fa	Ref. [32]	6.60
	Present model	6.56
	Error	0.60
R123	Ref. [32]	6.70
	Present model	6.67
	Error	0.44
R134a	Ref. [32]	6.45
	Present model	6.51
	Error	0.92

Table 3.
Validation results for VCC cycle.

5. Selection of the working fluid

The choice of the working fluid for an ORC or VCC cycle is an important criterion to improve the cycle performances. Generally, there are three families of organic fluids.

Figure 9 shows these three classes on a T-S diagram. The distinction between these different types essentially depends on the slope between the saturation temperature and the isentropic variation ($\Delta T/\Delta s$). If a negative slope is said, the fluid is wet, such as H_2O, NH_3, and R134a. For a positive slope, we speak of a dry fluid such as benzene and pentane. In cases where the slope is infinite, it is said that this fluid is isentropic like R600 and R600a.

For the ORC cycle is to have fluid hot admits a weak latent heat in the evaporator, in order to minimize the quantity received by the boiler. Thus, a low latent heat in the condenser minimizes the amount of cold delivered by the VCC cycle. In addition, we are looking for a fluid with a positive slope to avoid vapor having less than 0.95 of steam rate.

We guarantee the elimination of the oxidation effect in the turbine especially that we will make it lower concerning the condensation temperature to −10°C. Based on these criteria and conditions mentioned above, it is necessary to choose a dry or isentropic ORC cycle fluid. We choose the n-hexane; the chemical formula is C_6H_{14}. The thermophysical characteristics of this fluid are presented in **Table 4**.

The R600 is selected as a working fluid for the VCC cycle. It is a hydrocarbon of formula C_4H_{10} crude which is found in the gas status under normal conditions of temperature and pressure. The physical characteristics of this fluid are presented in **Table 4**. Furthermore, our choice is toward the use of n-hexane for the ORC cycle. This choice is essentially due to the steam rate which is equal to 1 even when the condensation temperature is lowered to a low degree. This allows us to have a margin of confidence and turbine safety (avoid the effect of oxidation). During our study, we chose the R600 as a working fluid for the VCC cycle. This fluid is characterized by its robustness in the market, so it is used in recent years in several researches. In addition, we find that the environmental damage is minimal.

6. System settings and boundary conditions

To reassure the efficiency and rentability of the system, it is necessary that we set some parameters and define their limits. For example, the network and

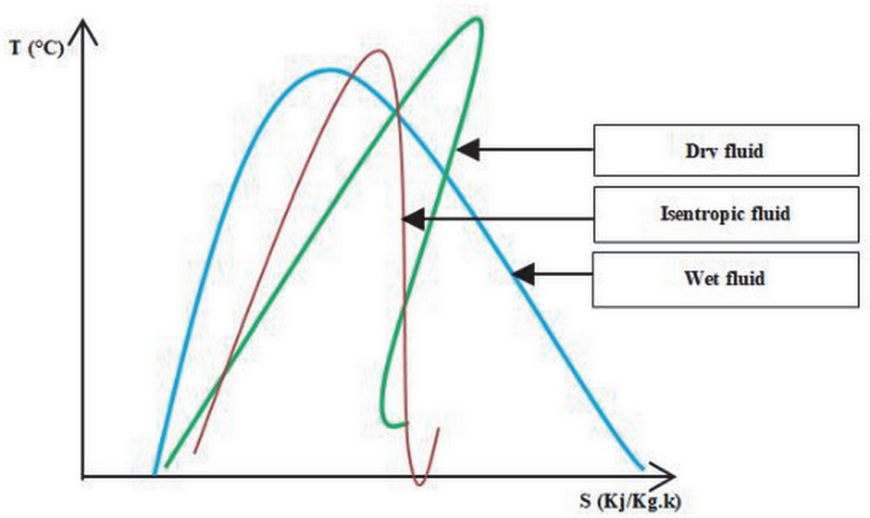

Figure 9.
The three classes on a T-S diagram.

Fluid	Critical temperature (°C)	Critical pressure (bar)	MW (kg/kmol)
Ammonia	132.3	113.3	17.03
R600a	134.7	36.4	58.12
R134a	101	40.59	102
R500	105.5	44.55	99.31
R236fa	124.9	32	152
Propane	96.68	42.47	44.1
R245fa	154	36.51	134
Acetone	235	47	58.08
n-Hexane	234.7	30.58	86.17
R600	152	37.96	58.12
R123	183.7	36.68	152.9

Table 4.
Physical and chemical property of work fluids.

refrigeration capacity must be always positive. Also, to guarantee the safety of the turbines, it is necessary that the vapors' quantity must be more than 95%.

The boundary conditions are shown in **Table 5**.

7. Results analysis and discussion

The main purpose of this study is to analyze the performance of a new system that combines the steam compression cycle and the Rankine cycle for tri-generation (electricity, cold, hot).

In the previous section, we presented the different designs of the system. This system has an energy autonomy. It needs only the solar temperature "T_h." For that reason, we will focus our work on the impact of solar temperature.

First of all, we started with the mass flow analysis of each circuit in order to have the mass potential of our mini power plant.

Figure 10 resumes the evaluation of the different values of the flow rate for each circuit. The different ratios of the mass flow rates are R_1, R_2, R_3, and R_4. The shape of different curves is of positive exponential form. It can be seen that the variation between the four curves is constant in function of T_h. The three ratios R_1, R_3, and R_4 represent small variations of the ratios of the flow rates as a function of T_h between them. Consequently, the geometries of different constituent bodies are coherent in terms of dimensions. In contrast, the ratio R_2 is a large margin of variation compared to the other ratios.

Wnet	>0
Qevnet	>0
X4	>0.95
$Tair_{in}$	30
$Tair_{out}$	18
T_6	30

Table 5.
Boundary conditions.

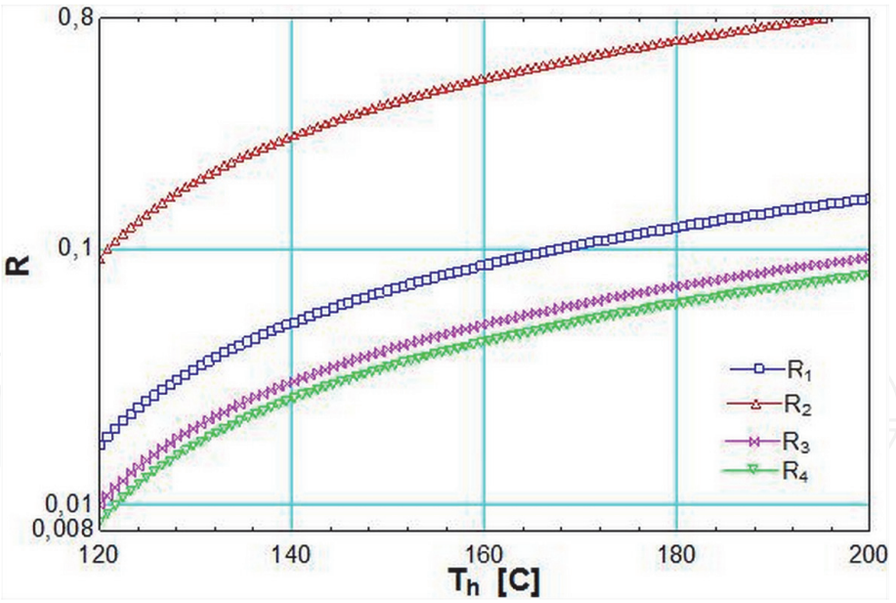

Figure 10.
The evolution of different throughput ratios as a function of T_h.

This variation in flow rates does not depend only on the temperature of the solar collector T_h, but it also depends on the temperature of the boiler T_g. For this, we have made surfaces of each flow ratio with two temperatures T_h and T_g as shown in **Figure 11**.

In addition, it can be noticed that the net quantity of the hot water is delivered by the system.

Figure 12 illustrates the evolution of different mass flow rates as a function of the heat delivered Q_b by the boiler. The four flows are varied proportionally with Q_b. It is

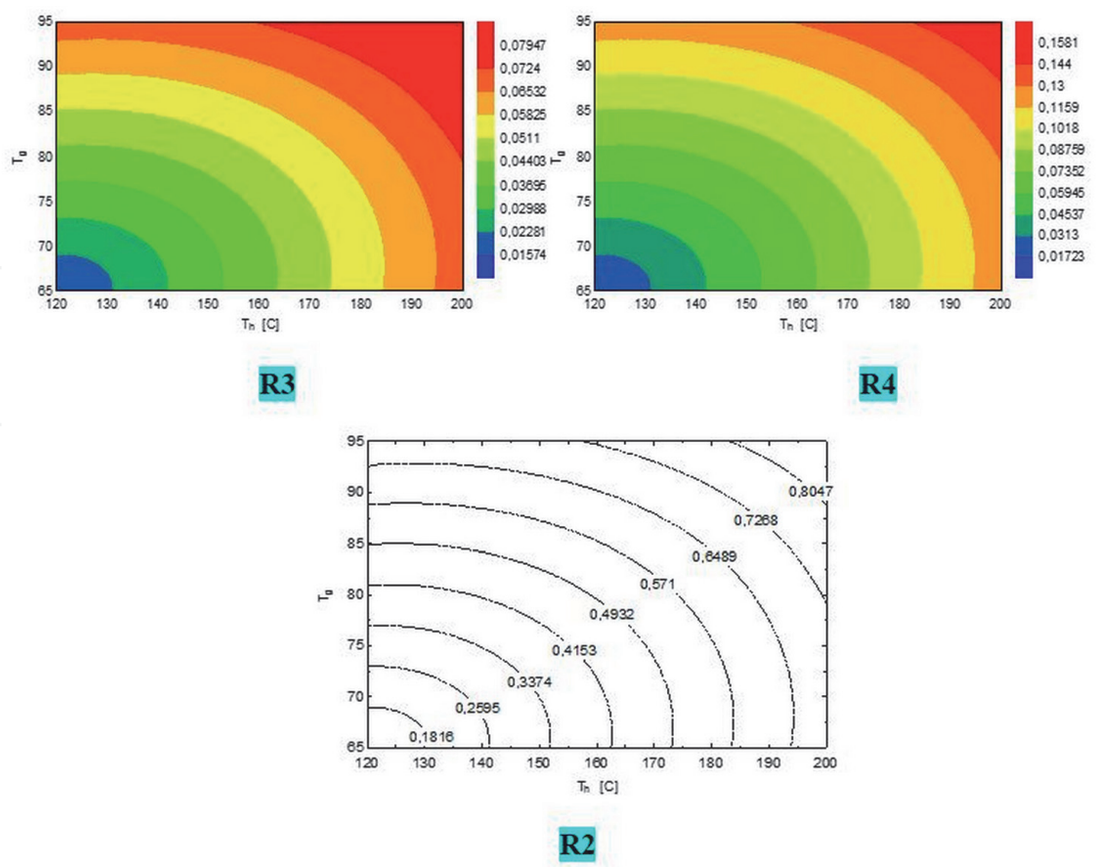

Figure 11.
Surfaces of flow reports as a function of each two temperatures T_h and T_g.

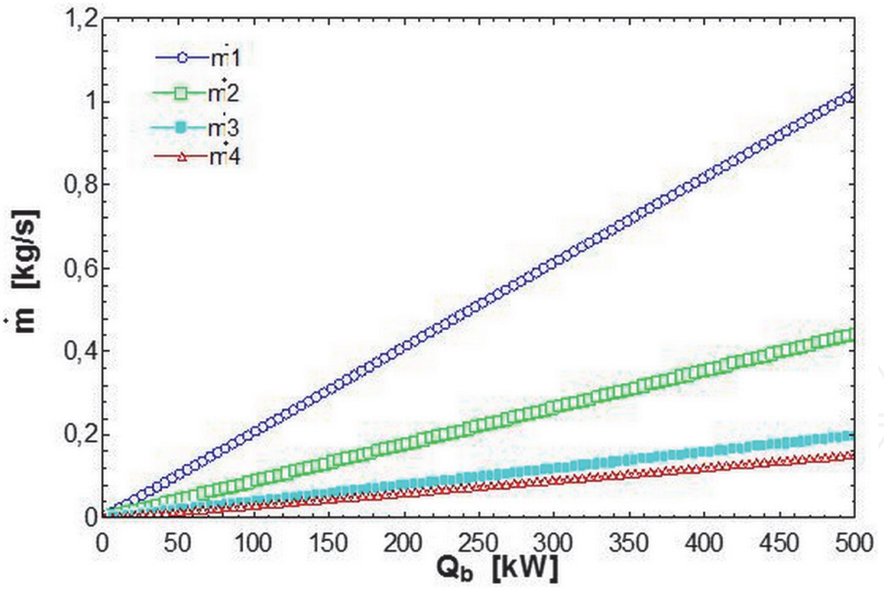

Figure 12.
The evolution of flows according to high-temperature heat source.

noted that the mass flow has a large positive slope with respect to the other mass flow rates. This allows us to interpret that the geometry of the ORC cycle is very important in relation to the different cycles. Also, this cycle promotes significant power.

It is constant that the lowest mass flow rate corresponds to the mass flow rate that does not exceed 0.18 kg/s, which means that the desalinated water is installed at a low power.

In energy potential term provided by our installation, **Figures 13** and **14** indicate the net work and the amount of cold produced as a function of the hot source Q_b. It is observed that the two quantities W_{net} and Q_{ev} are proportional to Q_b. It is possible to obtain a net work of maximum value equal to 14 kW and a maximum amount of cold equal to 75 kW.

Figure 15 shows the evolution of the ORC thermal efficiency as a function of the generator temperature T_g and the vaporization temperature of the cold T_{ev}.

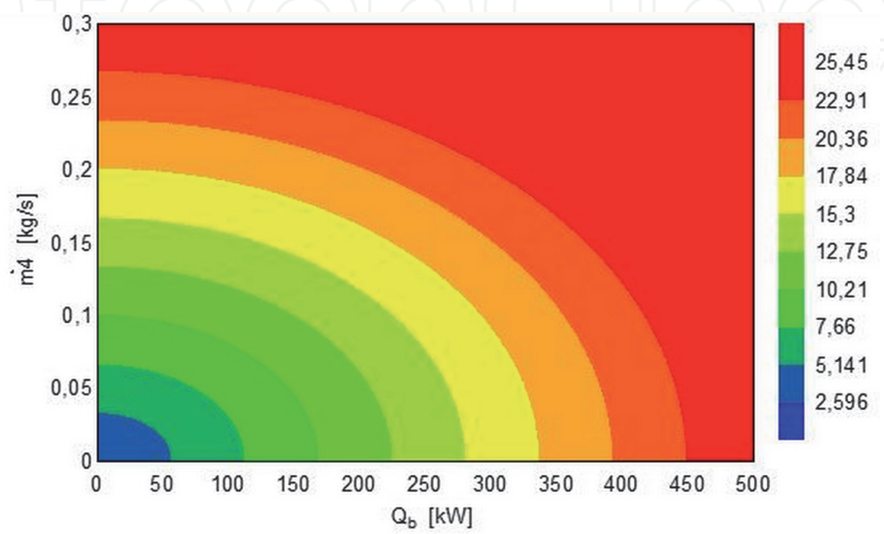

Figure 13.
The evolution of flows m_4 according to high-temperature heat source.

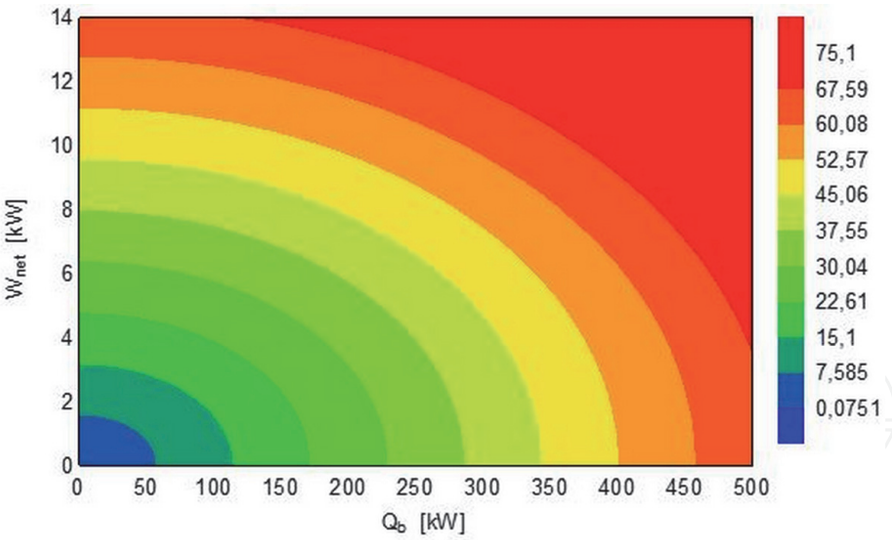

Figure 14.
Net work variation and cooling capacity according to Q_b.

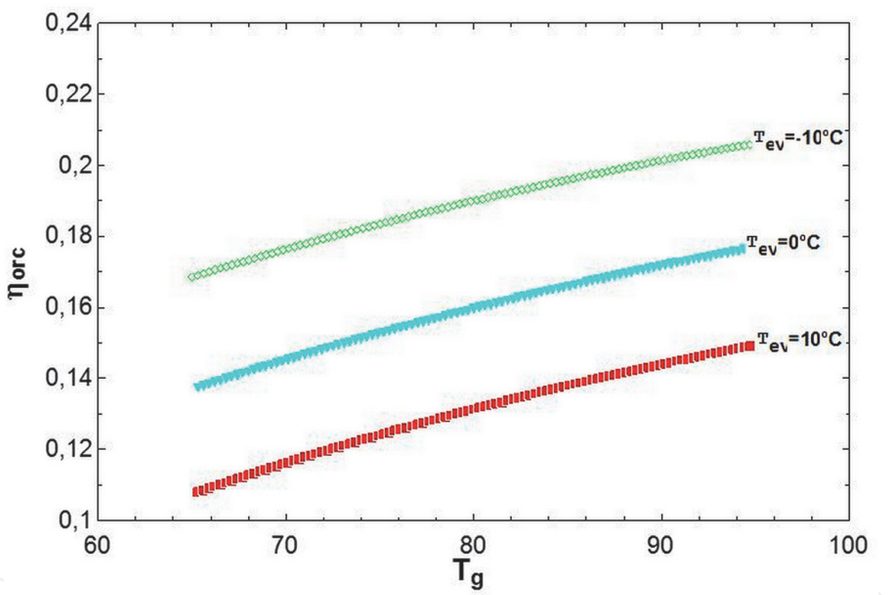

Figure 15.
Variation of ORC efficiency as a function of T_g and T_{ev} temperature.

It is observed that the ORC efficiency is proportional to T_g and inversely proportional to T_{ev}; this is justified by the first principle of thermodynamics. A better efficiency noted is 0.21 for $T_{ev} = -10°C$ and $T_g = 95°C$.

7.1 Technical-economic analysis and investment costs

The investment costs can be estimated from specialized works [30, 32–36] where they are generally presented in the form of charts or tables. Often these abacuses represent the cost taking into account the influence of parameters such as pressure, temperature, material or manufacturing, assembly, transport, etc.

We have undertaken to gather technical and economic data of the components used in the VCC and ORC cycles (compressors, condensers, evaporators) in order to

develop technical-economic and then exergo-economic con-elations. This task is not easy since often the data is discrete and the interpolations or extrapolations are not conclusive due to the nonlinearity of the cost according to the parameters used by the manufacturer.

7.1.1 Compressor cost

For compressors, the price depends on the type of compressor, the power, and the volume swept, while for motor compressors the price is given according to the type, the power, and flow of the heat transfer fluid at the condenser.

Compressor cost = f (type, power, volume swept).

Motor compressor cost = f (type, power, flow rate of the coolant at the condenser).

So for each model corresponding to a certain type of compressor, a function of the following form is established:

Compressor cost = a. (Power)^{b}. (Volume swept)^{c}

Determine the coefficients a, b, and c.

We are able to express by an analytical approach the price of a certain type of compressor, knowing the technical characteristics.

Generally correlations have been developed to determine the investment costs of each organ.

For the compressor, the correlations used are [37]:

$$ci_{\_CP} = 9.27.10^{-8} \; cyl^{(-4.85)} \; \dot{Q}_{EV}^{33} \; \dot{W}^{2}$$

with

$10.3 < cyl < 30.6$ [cm^3]

$835 < Q_{EV} < 2650$ [W]

$475 < W < 1225$ [W]

7.1.2 Evaporator cost

For evaporators the price depends on the type of evaporator, the power, the exchange surface, the flow of the heat transfer fluid at the evaporator, the number of fans, and the pitch of the fins.

Evaporator price = function (type, power, surface, flow, no. of fans, no fins).

For the evaporator, the correlations used are [37]:

$$ci_{\_EV} = 2.94 \; \dot{Q}_{EV}^{0.44} \; D_{EV}^{0.42}$$

with

$850 < Q_{EV} < 5500$ [W]

$685 < D_{EV} < 3325$ [m^3/h]

7.1.3 Condenser cost

The price of a condenser is given according to the type of condenser, the power, the exchange surface, the flow of heat transfer fluid, and the number of fans.

Price = function (type, power, surface area, heat transfer fluid flow, no. of fans).

For the condenser, the correlations used are [37]:

$$ci\_CD = 2.4.10^5 \ \dot{Q}_{CD}^{-0.53} \ D_{CD}^{1.96}$$

with
$3500 < Q_{CD} < 20{,}000$ [W]
$0.6 < D_{CD} < 2$ [m^3/h]

8. Conclusion

The energy performance of power and refrigeration cogeneration and trigeneration through an organic Rankine cycle (ORC) with a vapor compression cycle (VCC) by a new combination systematic is examined. We can use a low-temperature energy source. Two cases of refrigeration and cogeneration are analyzed, including cases of cogeneration (−10, 10°C) and congelation (0, −17°C).

The effects of the system parameters include the condensation and vaporization temperatures for ORC and VCC, and the efficiency E on performance such as thermal efficiency, specific refrigeration, and net work output and global system performance are investigated.

According to the analysis and the investigation carried out during this study, the main interpretations retained are:

- The results show that operating parameters have a significant effect on performance. This effect differs from one use case to another (positive or negative refrigeration) and according to the installed configuration (cycles A, B, and C).

- The three configurations developed which were based on the integration of recovery exchangers noted improvements in overall performance. These improvements also differ from one cycle to another, which makes it possible to say that the spot of integration of the exchangers is an effect on the performances.

- The results show that for cogeneration with negative cold, among the three configurations that we have developed, cycle B is preferable in which it has a better energy performance.

Nomenclature

COP_{vcc}	coefficient of performance for the vapor compression cycle
COP_s	coefficient of performance for the overall system
Ci_{cp}	investment cost of the compressor
Ci_{EV}	investment cost of the evaporator
Cyl	piston compressor displacement
Ci_{CD}	investment cost of the condenser
D_{CD}	heat transfer fluid flow rate at condenser
D_{EV}	heat transfer fluid flow rate at evaporator
H1	exchanger 1
H2	exchanger 2
H3	exchanger 3
+ H2. H1	cycle with exchangers 1 and 2

H	enthalpy (kJ/kg)
MW	molar mass
m_1	mass flow rate for ORC (kg/s)
m_2	mass flow rate for VCC cycle (kg/s)
m_3	mass flow rate for heated water
m_4	mass flow rate for seawater desalination
ORC	organic Rankine cycle
Pcrit	critical pressure
P_{sat}	saturated pressure
R_m	mass flow ratio
R_{pp}	pressure ratio for pump
R_{pc}	pressure ratio for compressor
T	temperature (°C)
T_{ev}	vaporization temperature for VCC cycle (°C)
T_{cit}	critical temperature (°C)
T_h	temperature in the panel solar (°C)
T_g	temperature in the boiler for ORC cycle
T_{cond}	condensation temperature for organic Rankine cycle
T_{sh}	overheating temperature for organic Rankine cycle
Q_b	boiler heat input (kW)
Q_{h2}	heat input for the exchanger 2 (kW)
Q_{ev1}	the power of the evaporator 1 (kW)
Q_{ev2}	the power of the evaporator 2 (kW)
Q_{ev}	the overall power evaporated by the VCC cycle (kW)
Q_{EV}	heat flow exchanged at the evaporator
Q_{CD}	heat flow exchanged at the condenser
VCC	vapor compression cycle
W_{com}	working fluid pump power consumption (kW)
W_{exp}	expander work output (kW)
W_{net}	net work output for overall system (kW)
W_{pump}	working fluid pump power consumption (kW)
W	compressor power
W_T	mechanical work of the turbine (KW)
Wc	mechanical work of the compressor (kW)
X	title vapor
η_{is1}	compressor isentropic efficiency
η_{is2}	expander isentropic efficiency
η_{pump}	working fluid pump isentropic efficiency
ΔT_{Pinch}	pinch temperature (°C)

Index

1	pump inlet
2	pump outlet
3	boiler output and expander inlet
4	expander outlet
10	compressor inlet
11	compressor outlet
11	condenser inlet
12	condenser outlet
13	evaporator 1 inlet
14	evaporator 1 outlet

DOI: http://dx.doi.org/10.5772/intechopen.91871

Author details

Noureddine Toujani*, Nahla Bouaziz and Lakder Kairouani
Energetic and Environmental Research Unity, National Engineering School of Tunis, Tunis El Manar University, Tunis, Tunisia

*Address all correspondence to: toujeninoureddine@gmail.com

References

[1] International Energy Agency (IEA). International Energy Outlook-Highlights. Washington DC, USA: IEA; 2010

[2] Mohanty S. Forecasting of solar energy with application for a growing economy like India: Survey and implication. Renewable and Sustainable Energy Reviews. 2017;**78**:539-553

[3] Nematollahi O. A feasibility study of solar energy in South Korea. Renewable and Sustainable Energy Reviews. 2017; **77**:566-579

[4] Ozoegwu CG. The status of solar energy integration and policy in Nigeria. Renewable and Sustainable Energy Reviews. 2017;**70**:457-471

[5] Sadiq AA, Dada Joseph O, Khalil AI. Current status and future prospects of renewable energy in Nigeria. Renewable and Sustainable Energy Reviews. 2015; **48**:336-346

[6] Herche W. Solar energy strategies in the U.S. utility market. Renewable and Sustainable Energy Reviews. 2017;**77**: 590-595

[7] Communication from the Commission to the European Parliament and the Council: "Energy Efficiency 610 and its contribution to energy security and the 2030 Framework for climate and energy policy"-Brussels, 611 23.7.2014 COM (2014) 520 final

[8] Sarbu I, Sebarchievici C. General review of solar-powered closed sorption refrigeration systems. Energy Conversion and Management. 2015;**105**: 403-422

[9] Gingerich DB, Mauter MS. Quantity, quality, and availability of waste heat from United States thermal power generation. Environmental Science and Technology. 2015;**49**:8297-8306

[10] Chen CL, Li PY, Le SNT. Organic Rankine cycle for waste heat recovery in a refinery. Industrial & Engineering Chemistry Research. 2016;**55**:3262-3275

[11] Sansaniwal SK, Sharma V. Energy and exergy analyses of various typical solar energy applications: A comprehensive review. Renewable and Sustainable Energy Reviews. 2018;**82**:1576-1601

[12] Bolaji B. Exergetic analysis of solar drying systems. Natural Resources. 2011;**2**(2):92-97

[13] Fudholi A, Sopian KB, Othman MY, Ruslan MH. Energy and exergy analyses of solar drying system of red seaweed. Energy and Buildings. 2014;**68**(Part A): 121-129

[14] Gunhan T, Ekren O, Demir V, Sahin AS. Experimental exergetic performance evaluation of a novel solar assisted LiCl–H_2O absorption cooling system. Energy and Buildings. 2014;**68** (Part A):138-146

[15] Siddiqui FR, El-Shaarawi MAI, SAM S. Exergo-economic analysis of a solar driven hybrid storage absorption refrigeration cycle. Energy Conversion and Management. 2014;**80**:165-172

[16] Bouaziz N, Lounissi D. Energy and exergy investigation of a novel double effect hybrid absorption refrigeration system for solar cooling. International Journal of Hydrogen Energy. 2015; **40**(39):13849-13856

[17] Gang P, Guiqiang L, Xi Z, Jie J, Yuehong S. Experimental study and exergetic analysis of a CPC-type solar water heater system using higher-temperature circulation in winter. Solar Energy. 2012;**86**(5):1280-1286

[18] Shukla SK, Gupta SK. Performance evaluation of concentrating solar cooker

under Indian climatic conditions. In: Proceedings of the Second International Conference on Energy Sustainability; Jacksonville, Florida, USA; 10–14 Aug, 2008

[19] Naik PS, Palatel A. Energy and exergy analysis of a plane reflector integrated photovoltaic-thermal water heating system. ISRN Renewable Energy. 2014; **2014**:9. Article ID 180618. DOI: 10.1155/2014/180618

[20] Wu J, Zhu D, Hua W, Zhu Y. Exergetic analysis of a solar thermal power plant. Advances in Materials Research. 2013;**724–725**:156-162

[21] Ehtiwesh IAS, Coelho MC, Sousa ACM. Exergetic and environmental life cycle assessment analysis of concentrated solar power plants. Renewable and Sustainable Energy Reviews. 2016;**56**:145-155

[22] Cau G, Cocco D. Comparison of medium size concentrating solar power plants based on parabolic through and linear Fresnel collectors. Energy Procedia. 2014;**45**:101-110

[23] Chang K-H, Lin G. Optimal design of hybrid renewable energy systems using simulation optimization. Simulation Modelling Practice and Theory. 2015;**52**:40-51

[24] Abedi S, Alimardani A, Gharehpetian G, Riahy G, Hosseinian S. A comprehensive method for optimal power management and design of hybrid RES-based autonomous energy systems. Renewable and Sustainable Energy Reviews. 2012;**16**:1577-1587

[25] Olatomiwa L, Mekhilef S, Ismail M, Moghavvemi M. Energy management strategies in hybrid renewable energy systems: A review. Renewable and Sustainable Energy Reviews. 2016;**62**: 821-835

[26] Torreglosa JP, García-Triviño P, Fernández-Ramirez LM, Jurado F. Control based on techno-economic optimization of renewable hybrid energy system for stand-alone applications. Expert Systems with Applications. 2016;**51**:59-75

[27] Dash V, Bajpai P. Power management control strategy for a stand-alone solar photovoltaic-fuel cell–battery hybrid system. Sustainable Energy Technologies and Assessments. 2015;**9**:68-80

[28] Zhou T, François B. Energy management and power control of a hybrid active wind generator for distributed power generation and grid integration. IEEE Transactions on Industrial Electronics. 2011;**58**:95-104

[29] Saleh B, Koglbauer G, Wendland M, Fischer J. Working fluids for low-temperature organic Rankine cycles. Energy. 2007;**32**:1210-1221

[30] Chauvel A et al. Manuel d'Evaluation Economique des Procédés. Paris: Edition Technip; 1976

[31] Nasir MY, Kim KC. Working fluids selection and parametric optimization of an organic rankine cycle coupled vapor compression cycle (ORC-VCC) for air conditioning using low grade heat. Energy and Buildings. 2016;**129**:378-395

[32] Chatelain C, Ducrocq JC, Mignard B, Coeytaux M. Optimisation technico-economique des processus énergétiques. Technique de l'Ingénieur, Génie Énergétique, B. 1996;**1282**:1-24

[33] Peters MS, Merhaus KD. Plant Design and Economics for Chemical Engineers. 4th ed. New York: McGraw Hill; 1991

[34] Garett DE. Chemical Engineering Economics. New York: Van Nostrand Reinhold; 1989

[35] Baasel WD. Preliminary Chemical Engineering Plant Design. 2nd ed. New York: Van Nostrand Reinhold; 1990

[36] Guthrie KM. Process Plant Estimating, Evaluating and Control. Solana Beach, CA, USA: Craftsman; 1974

[37] Lavinia GROSU. Contribution a l'optimisation thermodynamique et économique des machines a cycle inverse a deux et trois reservoirs de chaleur. Available from: http://www.cfcopies.com/V2/leg/leg_droi.php